Electronic Supplementary Material (ESI) for Lab on a Chip

Resolution enhancement of Suspended Microchannel Resonators for weighing of biomolecular complexes in solution

Mario M. Modena, Yu Wang, Dietmar Riedel, Thomas P. Burg

Supplementary Information

Autocorrelation fit function derivation

By using the Rayleigh-Ritz method, the frequency shift due to a single particle of mass m_p at axial position *x* can be expressed in terms of its maximum, $f_{p0} = -\frac{1}{2} f_0 \frac{m_p}{m^*}$, as

$$\Delta f_p(x) \approx f_{p0}\, u(x)^2, \tag{S1}$$

where $u(x)$ denotes the deflection function of the resonator normalized to amplitude 1 and the approximation is valid in the limit $m_p \ll m^*$ (m^* is the effective mass of the resonator). For simplicity of notation, the channel is mapped to a coordinate system in which the axial direction coincides with the *x*-axis and the cross section extends in the *yz*-plane (Figure S1).

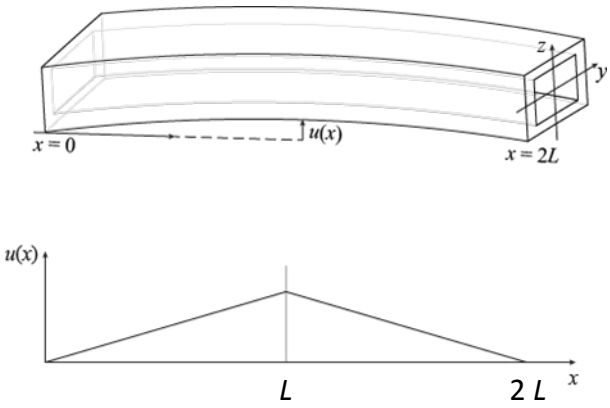

Figure S1. The embedded channel is mapped to a linear geometry in the calculations. The cross-section lies in the *yz*-plane, and the *x*-axis parameterizes the path along the channel axis. The deflection function of the torsional resonators used in this work is approximated as a linear function. The position $x = L$ corresponds to the apex of the paddle. The presence of two paddles is accounted for by an appropriate choice of the effective channel width, *W*.

The deflection function for the first vibrational mode of the torsional devices used in this work is well approximated by

$$u(x) = \begin{cases} x/L\,, & \text{for } 0 \le x \le L \\ (2L - x)/L\,, & \text{for } L < x \le 2L\,. \\ 0, & \text{otherwise} \end{cases} \tag{S2}$$

When multiple particles are simultaneously present in the sensing volume, the total frequency shift is to first order a linear superposition of the individual single-particle contributions. In the limit of large numbers, the local particle concentration can be expressed as

$$c(x, y, z, t) = c_0 + \delta c(x, y, z, t) \tag{S3}$$

where c_0 is the average concentration and δc describes the spatial and temporal fluctuations. The concentration fluctuations are converted into resonance frequency fluctuations as

$$\delta f(t) = f_{p0} \int_V \delta c(x, y, z, t) \cdot u(x)^2 dz\, dy\, dx. \tag{S4}$$

The autocorrelation of $\delta f(t)$,

$$C(\tau) = \langle\, \delta f(t) \cdot \delta f(t+\tau)\, \rangle, \tag{S5}$$

is therefore given by

$$C(\tau) = f_{p0}^2 \iint_V \langle \delta c(x,y,z,t)\delta c(x',y',z',t + \tau)\rangle\, u(x)^2\, u(x')^2 dy\, dz\, dx\, dy' dz' dx'. \tag{S6}$$

To arrive at an approximation for $C(\tau)$ that accounts for the velocity distribution in a rectangular channel, the cross-sectional parts of the double volume integral are discretized into *M* compartments of area A_i (*i* = 1 … *M*). Assuming that the concentration fluctuations in different compartments are uncorrelated, one can write

$$C(\tau) = \sum_{i=1}^{M} C_i(\tau). \tag{S7}$$

Within each compartment, the flow profile is approximated as plug flow of velocity v_i, and any exchange of particles between compartments by diffusion is neglected. The functions $C_i(\tau)$ are given by

$$C_i(\tau) = f_{p0}^2 \iint_{V_i} \langle \delta c(x,y,z,t)\delta c(x',y',z',t + \tau)\rangle\, u(x)^2\, u(x')^2 dy\, dz\, dx\, dy' dz' dx', \tag{S8}$$

which can be evaluated directly using the concentration correlation function for uniform flow in the x-direction:

$$\langle \delta c(x,y,z,t)\delta c(x',y',z',t+\tau)\rangle = c_0\, \delta(x - x' - v_i\, \tau)\, \delta(y - y')\, \delta(z - z'). \tag{S9}$$

Here $\delta(x)$ denotes the Dirac delta function. The scaling by c_0 reflects the assumption that the particle number fluctuations in a fixed volume of solution follow a Poisson distribution. Equation S8 then yields

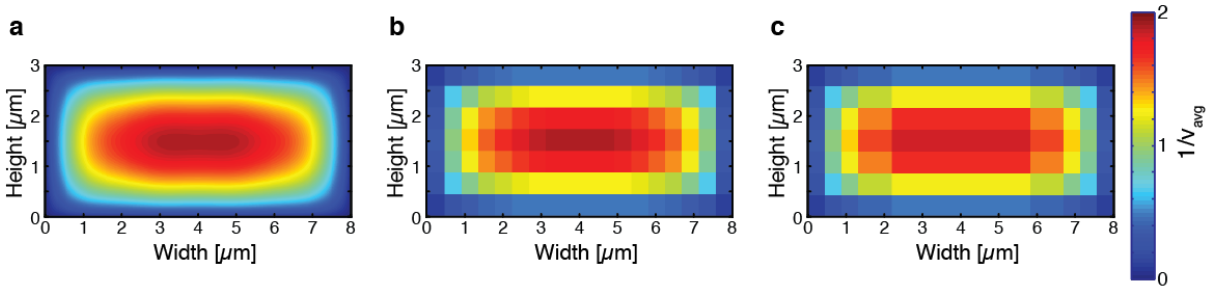

Figure S2. Velocity profile in the microfluidic channel. a) Velocity profile calculated with the *Spiga and Morini*[1] method, n and m truncated to 7; b) approximation of the velocity profile in 36 streams of ~450x450 nm^2. The streams better represent the actual particle velocity distribution because of lateral diffusion; c) merging of streams of similar velocity in the x-direction for simplifying the autocorrelation fit function. All plots are normalized to the average velocity.

$$C_i(\tau) = f_{p0}^2\, c_0\, A_i \int_0^{2L} u(x)^2\, u(x - v_i\,\tau)^2\, dx, \tag{S10}$$

with the integral

$$g(s) \equiv \int_0^{2L} u(x)^2\, u(x-s)^2\, dx$$

$$= \begin{cases} L \cdot \left[\frac{1}{30}\left(2-\frac{|s|}{L}\right)^5 - \frac{2}{3}\left(1-\frac{|s|}{L}\right)^4\right], & |s| \le L \\ L \cdot \frac{1}{30}\left(2-\frac{|s|}{L}\right)^5, & L < |s| \le 2\,L \\ 0, & otherwise \end{cases} \tag{S11}$$

The flow velocity profile in the embedded channel is calculated according to the formulation of *Spiga and Morini*[1]

$$v(\bar{y},\bar{z}) = \frac{16\,\beta^2}{\pi^4} \sum_{n\ odd}^{\infty} \sum_{m\ odd}^{\infty} \frac{\sin(n\pi\bar{y})\,\sin\,(m\pi\bar{z})}{nm(\beta^2 n^2 + m^2)}, \tag{S12}$$

where $\bar{y}$ and $\bar{z}$ are the normalized cross section dimensions ranging from 0 to 1 and β is the channel aspect ratio (in our case 3/8). For the calculations, n and m were limited to 7.

The number of compartments used in Equation S7 may be chosen so as to partially account for the effects of particle diffusion and finite particle size, as we now explain. Particles that

undergo diffusion are able to cross between streamlines, thereby changing their velocity. To account for this effect, the size of the compartments was chosen of the same order of magnitude as the diffusion length scale corresponding to the average passage time, as shown in Figure S2. Considering a sample of 100 nm transiting through the resonator in 50 ms, and rounding to an integer number of streams in the cross section, we set the bin dimensions to ~450 x 450 nm^2, obtaining 36 streams. As the velocity profile can be considered constant for a large section along the y-dimension, adjacent streams with similar velocities can be merged without affecting the velocity particle distribution. The number of streams can be reduced to 20, simplifying the fit function.

The approximation to a straight model neglects the cross section widening and the flow profile variation at the corners, which might cause small inaccuracies in the autocorrelation shape. However, the goodness of the fits to the experimental data indicates that the shape error is likely to be smaller than the noise measurement.

Another important difference between a straight and a U-shaped channel is due to the variation in particle axial position when crossing the cantilever apex, that causes uncertainties on the single particle mass measurement[2]. However, this source of uncertainty does not affect the mass estimation when analyzing the results with the autocorrelation method. Because of the symmetry of the velocity profile in the channel, each streamline causing a positive variation in the mass estimates is matched by a streamline with an opposite contribution. Therefore, this effect causes at first order a zero net uncertainty contribution in the autocorrelation analysis.

Mass responsivity calibration

In order to control the flowing conditions in the resonator and to characterize the mass-frequency response of the device, a known concentration of reference particles was added to each sample before measurements. The reference particles were NIST 1.54 µm polystyrene particles (Polysciences Inc, Eppelheim, Germany) in aqueous solution. The 1% w/v stock concentration was diluted in the sample buffer to the wanted working concentrations, not to affect the sample conditions.

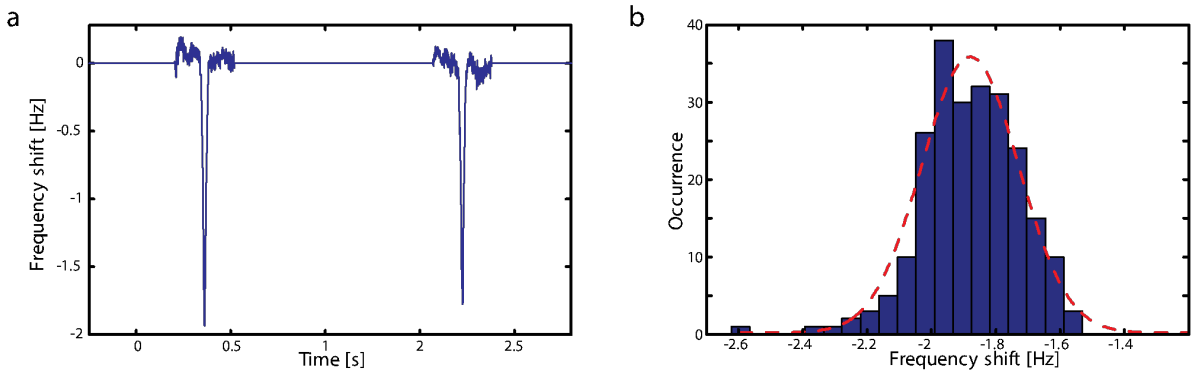

Figure S3. Reference particle signature and distribution. a) Two reference particle signatures extracted from the time domain trace. As the induced frequency shift clearly exceeds the measurement noise, single-particle detection can be carried out with high resolution. The mass-frequency conversion found for these particles was used as calibration for the resonator mass responsibity; b) histogram of the maximum frequency shifts caused by the reference particles and Gaussian fitting (in red). Mean and standard deviation of the Gaussian fit were used to characterize the mass responsivity of the device.

Because of their high buoyant mass (~100 fg in H_2O), the reference signatures are clearly

visible in the time domain trace (Fig. S3a). These signatures were detected and computationally excluded from the data used in the correlation analysis. Fig. S3b shows a histogram of the reference particle maximum frequency shifts detected during the 85 nm polystyrene measurements. As the mass of the particles is known, the frequency measurements are used for characterization of the resonator mass responsivity. Therefore, the uncertainty in the measurement is translated in uncertainty on the absolute mass calibration, but does not affect relative differences between measurements.

The presence of multiple embedded channels improves the signal-to-noise ratio of the measurement by increasing the measurement volume. However, in the event of clogging of one of the channels, the decrease of total flow through the resonator would cause a reduction in local concentration fluctuations, leading to an underestimation of the particle buoyant mass during data analysis. However, if the flow conditions are stable and consistent during the measurements, this error only affects absolute mass estimation, but relative comparisons between samples are conserved.

85 nm polystyrene particle measurements

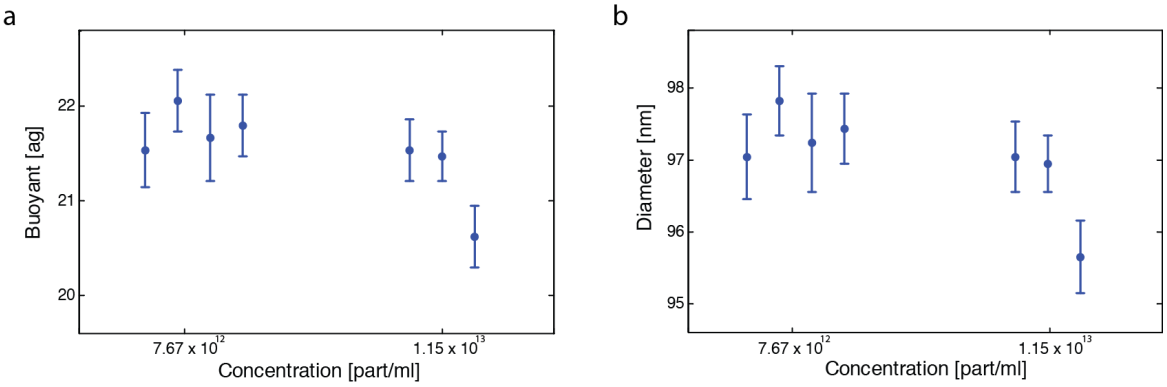

Figure S4. 85 nm polystyrene particles measured at two sample concentrations and under different flowing conditions. a) Buoyant masses obtained for the different measurement conditions; b) radius of the particles, calculated considering a buffer solution with density of 1.005 g/cm^3 and polystyrene density of 1.05 g/cm^3. The error bars show the propagated statistical error of the fitting parameter on the calculation of buoyant mass and particle radius.

To characterize the repeatability of the measurement, two samples of 85 nm polystyrene particles (Polysciences Inc, Eppelheim, Germany) were measured at different concentrations and flowing conditions. The stock solution (2.6% w/v in aqueous buffer) was diluted in 100 mM NaCl, 350 µM SDS, 0.01% w/v NaN_3 to 0.25% w/v (7.57 x 10^{12} part/ml) and 0.38% (1.15 x 10^{13} part/ml) concentrations. The flow conditions, for both concentration, were varied to obtain measurements with average residence times in the cantilever ranging from 20 ms to 150 ms. This range of transit times was selected to ensure that the slow variations (<1 Hz) due to

thermal drift and vibrations could be filtered out reliably in the data analysis.

Fig. S4a shows the measured buoyant mass for each measurement, using as calibration standard the 1.54 µm NIST polystyrene particles, and buffer density 1.005 g/cm^3. Knowing the density of polystyrene, 1.05 g/cm^3, it was possible to calculate the radius of the particles, and the results are plotted in Fig. S4b.

Insulin Aggregation Measurements

Here reported are the fit parameters of the curves plotted in Fig. 4a. The flow-through average times have been used to normalize autocorrelation functions, for comparing the curves taken at different time points.

Time point [hours]	**Amplitude** [Hz^2]	**Average transit time** [ms]
0	(3.0±0.8)x10^{-5}	232±84
2	(4.5±0.8)x10^{-5}	248±65
3	(5.91±0.61)x10^{-5}	126±18
4	(18.0±1.1)x10^{-5}	107±9
5	(24.5±0.8)x10^{-5}	140±6
6	(108±2)x10^{-5}	83±2
7 ½	(331±2)x10^{-5}	135±1
8 ½	(580±5)x10^{-5}	110±1

EM micrographs of insulin fibrils

Non-sonicated

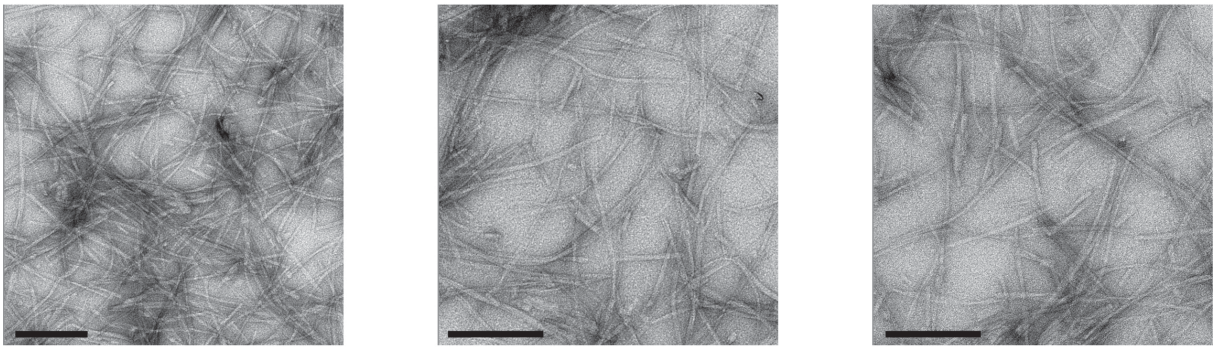

Sonicated

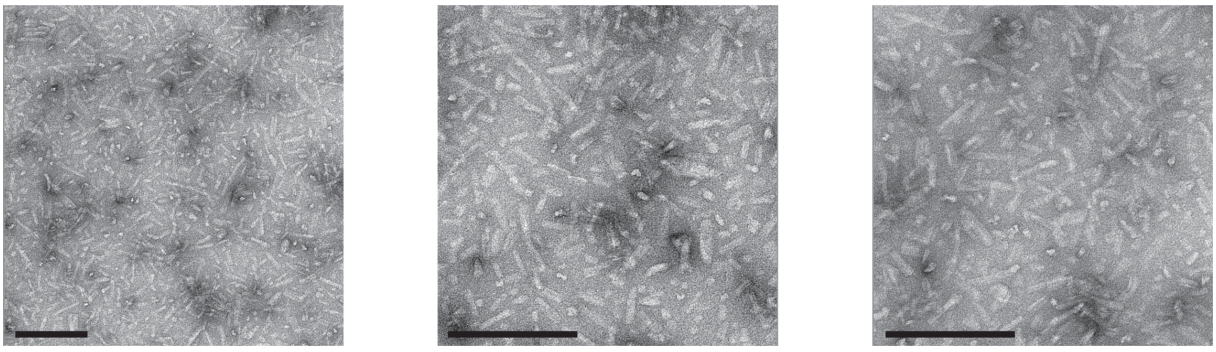

Fig S5. EM micrographs of the insulin fibrils after 8 ½ hours of incubation, before and after ultrasonication. Scale bars 200 nm.

The EM images in Figure S5 clearly show the fragmentation of amyloid fibrils upon ultrasonication. Fibrils after 8 ½ hours of aggregation present a wide length distribution and are, qualitatively, ~300 nm long. After sonication, their distribution looks more monodisperse, with an average length <<100 nm. These values are in good accordance with the estimates obtained with the mass correlation analysis (308±24 nm before sonication and 50±4 nm after sonication).

1. Spiga, M. & Morini, G. L. A symmetric solution for velocity profile in laminar flow through rectangular ducts. *International Communications in Heat and Mass Transfer* **21,** 469–475 (1994).
2. Lee, J., Bryan, A. K. & Manalis, S. R. High precision particle mass sensing using microchannel resonators in the second vibration mode. *Review of Scientific Instruments* **82,** 023704 (2011).